A FINITE ELEMENT SURFACE IMPEDANCE REPRESENTATION FOR STEADY-STATE PROBLEMS

A. J. KALINOWSKI

NAVAL UNDERWATER SYSTEMS CENTER
NEW LONDON, CONNECTICUT 06320

SUMMARY

A procedure for determining the scattered pressure field resulting from a monochromatic harmonic wave that is incident upon a layered energy absorbing structure is treated. The situation where the structure is modeled with finite elements and the surrounding acoustic medium (water or air) is represented with either acoustic finite elements--or--some type of boundary integral formulation, is considered. Finite element modeling problems arise when the construction of the structure, at the fluid-structure interface, are nonhomogeneous and in particular when the inhomogeneities are small relative to the acoustic wave length. An approximate procedure is presented for replacing the detailed microscopic representation of the layered surface configuration with an equivalent simple surface impedance finite element, which is especially designed to work only at limited frequencies. An example problem is presented using NASTRAN, however the procedure is general enough to adapt to practically any finite element code having a steady state option.

INTRODUCTION

This paper addresses the topic of solving acoustic-structure interaction problems involving a configuration having some sort of soft layered viscoelastic material, applied to a stiffer main body. Typically, acoustic sound energy impinges upon the treated structure (e.g. Figure 1a) and it is of interest to determine the reflected acoustic pressure. Specifically, the finite element method of solution is considered for the representation of the acoustically surface treated structure, and either acoustic finite elements (ref. 6,7)--or--some type of boundary integral method (ref. 8) that does not directly involve modeling the fluid is considered for the fluid. For either type of fluid representation there still remains the difficult problem of representing the energy absorbing properties of the viscoelastic outer layer in cases where the microscopic details are too complicated to represent with finite elements in the practical case where a large region of the structure is to be analyzed. On the other hand if only a small patch of the structure were

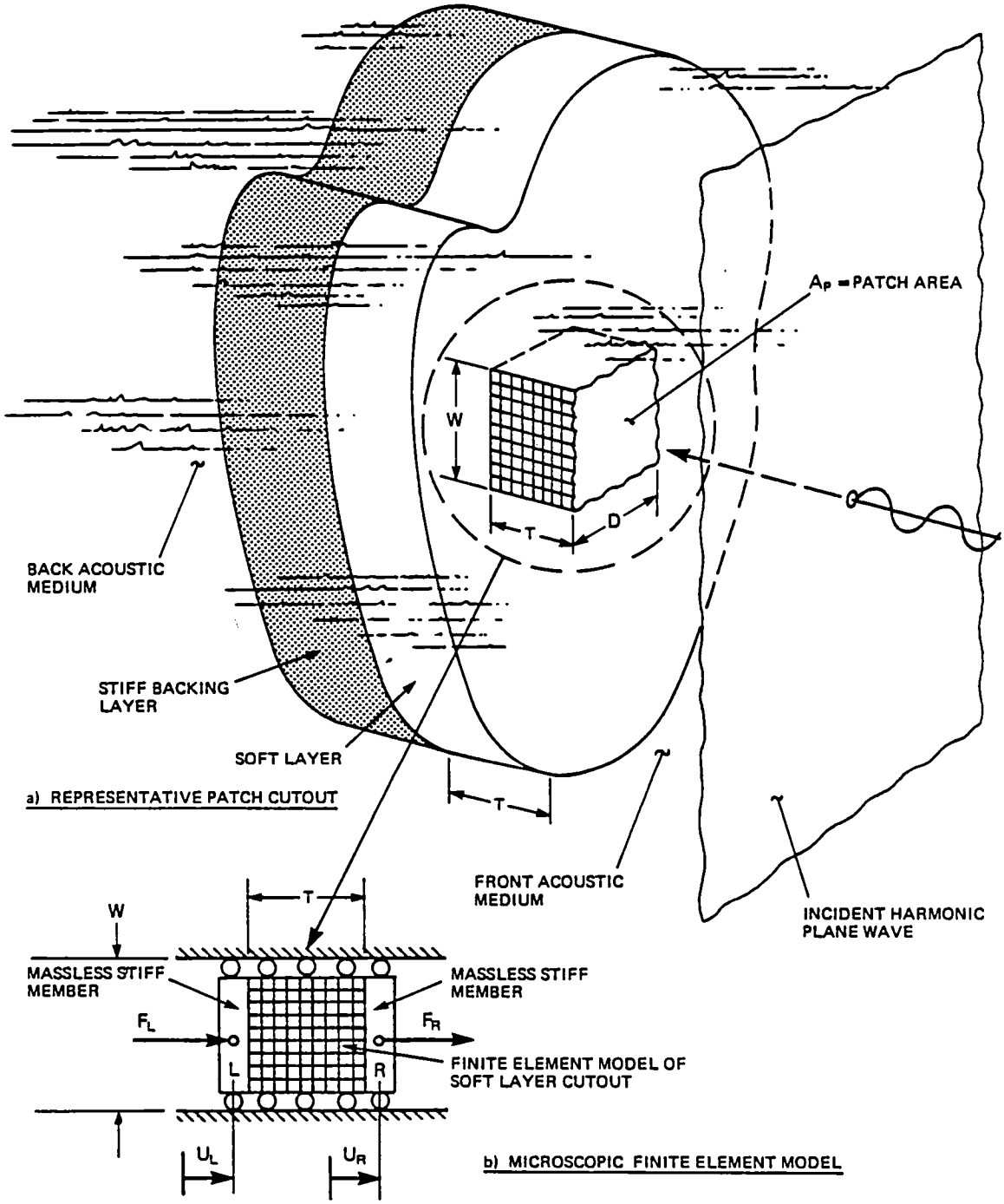

FIGURE - 1 GENERATION OF MACRO DYNAMIC STIFFNESS ($\bar{K}$)

considered of, say, area A_p (see Figure 1a), it would be well within the range of practical finite element analysis.

The idea pursued here is to use this microscopic patch, in some sense, to generate a super finite element with many less degrees-of-freedom as the detailed microscopic patch, yet produces nearly the same reflected pressure field had the main body been entirely been modeled with the detailed finite element representation. Essentially the finer details of the soft nonhomogeneous layer are smeared out and represented by a sequence of simplier macroscopic elements. Conceptionally, the Figure 1a configuration is replaced by the simplier finite element model shown in Figure 2, where the concept is generalized to apply to a curved surface. In Figure 2, the details of the stiff backing layer are not shown and are left as a choice to the model maker whether to represent the backing structure with say plate elements or solid brick elements. A choice of which acoustic fluid representation (i.e. finite element or boundary integral method) must also be made. The remainder of this paper focuses on the problem of defining the properties of the microscopic viscoelastic nonhomogeneous layer by specifically prescribing an equivalent macroscopic lumped parameter element of the type shown in Figures 3 and 4.

Obtaining an approximate simplier model to represent a more complex nonhomogeneous viscoelastic layer has been considered by others, refs. (1-5). However in these earlier works, particularly ref. (1 and 5), the emphasis was concerned with obtaining a simple lumped parameter representation of the layer directly in terms of the identifiable physical parameters of the layer (e.g. modulus of elasticity and thickness) so that the physics of the layer's acoustical performance could be explained. In contrast, for the work presented here, we use the lumped parameter only as a means towards fitting the actual microscopic surface impedance, and the meaning of the lumped parameters need not be related to any specific physical properties of the nonhomogeneous layer. Further, in none of the referenced works (1-5), has an attempt been made to apply the results of the work to some sort of finite element scheme such as in Figure 2.

OUTLINE OF THE METHOD

Before proceeding to the detailed development, a brief outline of the procedure is helpful. The first step is to cut out a representative patch, of surface area, A_p, from the overall configuration, such as the one shown in Figure 1a. Next a detailed finite element model of the patch is constructed, like shown in Figure 1b, where from this finite element model of the soft nonhomogeneous layer alone, we can obtain the smeared out macroscopic dynamic stiffness. Next, through a curve fitting process, an equivalent simple lumped parameter finite element model is designed that has the same surface impedance as the finite element patch at only one frequency (for the Figure 3 model) or at only two frequencies (for the Figure 4 model). Next the simple lumped parameter elements are distributed over the whole surface of the structure (e.g. Figure 2), where the same lumped parameters are used for all surface nodes, except for an alteration accounting for the fact that the surface area, A_n, around each node might be different if a variable mesh is used. The fact

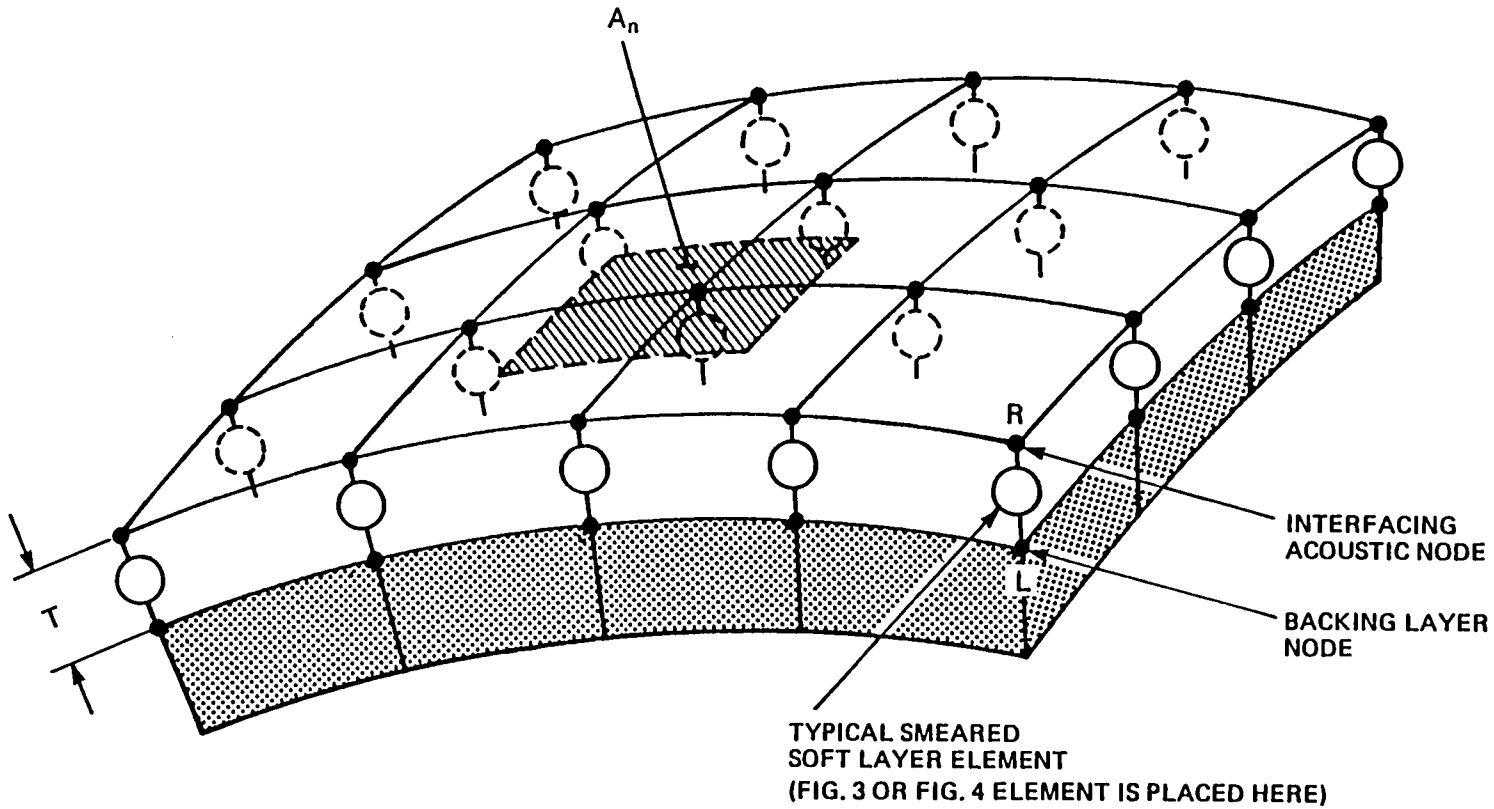

FIGURE - 2 SINGLE ELEMENT SMEARED MACROSCOPIC REPRESENTATION OF SOFT LAYER

that the direction of the normal to the surface changes on a curved surface is treated automatically when the bar version (NASTRAN CONROD) of the lumped parameter model (Figure 3C or Figure 4C) is used. Finally, the fluid is connected to the fluid side terminals of the lumped parameter elements (either acoustic finite elements--or--the boundary integral interaction matrix), and the scattering problem is solved in the usual manner for scattering from a homogeneous elastic body (e.g. using NASTRAN rigid format 8 with the acoustic elements of ref. 6 or 7 as appropriate and absorbing radiation boundary of ref. 9).

MACROSCOPIC IMPEDANCE DETERMINATION

The first step is to obtain the macroscopic surface impedance of a small patch of the actual nonhomogeneous viscoelastic layer. The methodology given here is general enough to treat a variety of inhomogeneities ranging from the tubes of ref. (3) to the imbedded voids used in refs. (2) and (5). Therefore in what follows, we are not specific about the layer, wherein the only requirement is that the patch size, A_p, is just large enough to pick up a typical repeated pattern. The Figure 1a, shows the sample patch as a WxD rectangular one, however, the shape should be whatever is convenient to represent the repeated pattern. Figure 1b shows a generic finite element representation. It is important to point out that the details of the finite element model must be fine enough to properly represent the complex spatial response existing within the layer. It is further assumed that the Figure 1a viscoelastic layer is infinite in extent and that plane of symmetry type boundary conditions can be applied to all four lateral faces (of areas WxT and DxT). This boundary condition is represented by the zero lateral constraint indicated by the rollers shown in Figure 1b.

The Figure 1b model is designed to respond to normal pressure that is approximately uniform over the patch surface. To obtain the smeared effects of the inhomogeneities, a weightless rigid "piston like" member is attached to the left and right surfaces of the layer (hence the designation L and R to denote the left and right surface nodes and all other pertinent surface related items). The attachment of the pistons to the layer is a rigid connection in the normal direction of motion, however the lateral direction attachment depends on the specifics of the application. The usual case is also a rigid attachment in a direction transverse to the motion direction on the left side (attachment to stiff backing structure), where as the attachment can allow transverse slip on the right side (attachment to the fluid). Double nodes are required when such slip is allowed.

The relationship relating the left and right piston faces and displacements are given by

$$\underset{\{F\}_B}{\begin{Bmatrix} F_L \\ F_R \end{Bmatrix}} = \underset{[\bar{K}]_{2x2}}{\begin{bmatrix} \bar{K}_{LL} & \bar{K}_{LR} \\ \bar{K}_{RL} & \bar{K}_{RR} \end{bmatrix}} \underset{\{U\}_B}{\begin{Bmatrix} U_L \\ U_R \end{Bmatrix}} \qquad (1)$$

where the forces, F_L and F_R, on the left and right piston vary harmonically according to

$$F_L = \bar{F}_L \exp(i\omega t), \quad F_R = \bar{F}_R \exp(i\omega t) \tag{2}$$

and the piston displacements U_L, U_R according to

$$U_L = \bar{U}_L \exp(i\omega t) \quad U_R = \bar{U}_R \exp(i\omega t) \tag{3}$$

The 2x2 dynamic stiffness, $[\bar{K}]$, which is the coefficient of $\{U\}_B$ in equation (1), can be computed from the fundamental matrices $[K]$, $[M]$, and $[C]$ of the figure (1b) microscopic finite element model by decomposing the response into boundary nodes (B subscripts) and interior nodes (I subscripts). Thus

$$\begin{Bmatrix} F_B \\ \hline F_I \end{Bmatrix} = \underbrace{\left[\begin{array}{c|c} K_{BB} & K_{BI} \\ \hline K_{IB} & K_{II} \end{array}\right]}_{[\bar{K}]_T} \begin{Bmatrix} U_B \\ \hline U_I \end{Bmatrix} \tag{4}$$

can be used to solve for $\{F\}_B$ in terms of $\{U\}_B$, (note that $\{F\}_I = \{0\}$ since there are no forces on the internal nodes), where the elements of $[\bar{K}]$ are of the form

$$[\bar{K}]_T = (-[M]\omega^2 + [K] + i\omega [C])$$

It follows that after eliminating $\{U\}_I$ from (4), we obtain

$$\{F\}_B = [\bar{K}_{BB} - \bar{K}_{BI} \bar{K}_{II}^{-1} \bar{K}_{IB}]\{U\}_B \tag{5}$$

and comparing equations (1) and (5), it is evident that $[\bar{K}]$ can be computed from

$$[\bar{K}] = [\bar{K}_{BB} - \bar{K}_{BI} \bar{K}_{II}^{-1} \bar{K}_{IB}] \tag{6}$$

Therefore, one approach to obtaining the $[\bar{K}]$ representation of the microscopic layer at some desired frequency, say ω_1, would be to evaluate $[\bar{K}]$ by constructing the right hand side of equation (6) with a DMAP sequence of instructions. This however is an unwieldly process which involves both partitioning the microscopic $[\bar{K}]_T$ matrix (e.g. ref. 10) and forming the inverse of $[\bar{K}]_{II}$, which could be a costly process.

An alternate process for generating $[\bar{K}]$ is to compute it directly from two finite element runs, involving the Figure 1b patch model. For a single frequency ω_1, we need to solve for the four complex constants comprising $[\bar{K}]$ in equation (1). These four constants are generated from the following two finite elements runs which are referred to as computer "run-a" and "run-b"

- "run-a"; set $\bar{F}_L^a = 1.0$, $\bar{U}_L^a = 0.0$, compute $\bar{U}_L^a$, $\bar{F}_R^a$ from NASTRAN "run-a"

NOTE: Superscripts a and b refer to "run-a" and "run-b"

"run-b"; set $\bar{F}^b_R = 1.0$, $\bar{U}^b_L = 0.0$, compute

$\bar{U}^b_R$, $\bar{F}^b_L$ from NASTRAN "run-b"

Where the complex forces, $\bar{F}^a_R$ and $\bar{F}^b_L$ are read from the forces of constraint printout as activated by the presence of SPCFORCES = ALL card in the case control in the case of NASTRAN. The $\bar{U}^a_L$ and $\bar{U}^b_R$ complex displacement amplitudes are part of the normal finite element output as activated by the DISPLACEMENT = ALL card. Inserting the results of these two runs directly into equation (1) gives four equations and four unknowns to determine the four complex stiffness entries of the 2x2 $[\bar{K}]$ matrix, namely

$$[\bar{K}(\omega)] = \begin{bmatrix} \frac{1}{\bar{U}^a_L} & \frac{\bar{F}^b_L}{\bar{U}^b_R} \\ \frac{\bar{F}^a_R}{\bar{U}^a_L} & \frac{1}{\bar{U}^b_R} \end{bmatrix} \equiv \begin{bmatrix} \left(\bar{K}^r_{LL} + \bar{K}^i_{LL}\right) & \left(\bar{K}^r_{LR} + i\bar{K}^i_{LR}\right) \\ \text{SYMM} & \left(\bar{K}^r_{RR} + i\bar{K}^i_{RR}\right) \end{bmatrix} \quad (7)$$

where the matrix $[\bar{K}]$ is symmetric. The response and constraint forces will in general be complex when the microscopic finite element model of Figure 1b consist of materials having viscoelastic dissipation (this effect is activated by the GE parameter on a NASTRAN MAT1 card). For each frequency, ω, there are six numbers $\bar{K}^r_{LL}$, $\bar{K}^i_{LL}$, ... $\bar{K}^i_{RR}$ that define the smeared macroscopic stiffness. Upon repeating the process described to generate equation (7) over a sweep of frequencies, a frequency description of the smeared macroscopic stiffness can be obtained like the one illustrates in Figure 6. Using the frequency sweep option in NASTRAN, the data used to generate the Figure 6 example was generated with just two computer runs, by frequency sweeping the two "run-a", "run-b" cases described earlier.

LUMPED PARAMETER ELEMENTS

The three complex terms in equation (7) define the equivalent dynamic stiffness for a patch of area A_p normal to the surface, in a global coordinate system with one coordinate axis also in line with the normal to the surface. There now remains the task of implementing equation (7) as an element in the finite element code, so that the as yet undefined layer elements shown in Figure 2 can be implemented. Two basic lumped parameter models are developed herein. The first one is a single frequency model, that is designed to represent equation (7) only at one selected frequency. The second model is similar, except it is designed to represent equation (7) at two selected frequencies. Further, the second model automatically interpolates between the two selected frequency and therefore attempts to represent the nonhomogeneous layer response over a limited hand of frequencies. The area of the patch, A_p, used to generate the macroscopic stiffness of equation (7) is in general, different from the area factor, A_n, used to convert distributed loads into concentrated nodal forces (see Figures 2 for A_n). Consequently, the generalized stiffness per unit patch area $(1/A_p)[\bar{K}]$ is a more fundamental quantity to work with. The dynamic stiffness to use at a typical node

connection shown in Figure 2 then would be

$$[\tilde{K}] = (A_n/A_p)[\bar{K}] \tag{8}$$

Implementation of $[\tilde{K}]$ in the finite element code is awkward, although straight forward, when the element is not in alignment with one of the axis of the global coordinate system. In this case, equation (8) is further modified with a coordinate transformation

$$[\tilde{K}]' = [T]^T[\tilde{K}][T] \tag{9}$$

where $[T]$ is the usual local to global coordinate transformation used in rod finite elements (ref. 11).

The implementation of equation (9) directly might require some sort of preprocessor, to generate the $[\tilde{K}]'$ matrix in conjunction with the coordinate transformations. A simplier alternate procedure is also given, that redefines the local $[\bar{K}]$ matrix in terms of rods (tension members such as CONROD and CVISC elements in NASTRAN), and the existing machinery in the finite element code will automatically take care of any transformations. Still another way to treat the coordinate transformation is to let each node have its own coordinate system, where one of the axis is aligned along the normal to the surface. This can be invoked in NASTRAN via a CORD1R card. In this manner, NASTRAN would automatically take care of the transformations, however it would require every node to have its own coordinate system.

Single Frequency Lumped Parameter Element

Here we are concerned with implementing equation (7), to each surface node (e.g. as in Figure 2), but we only require that the analysis be done at one frequency, ω_1. We give three alternate methods of installing the appropriate nodal dynamic stiffness.

a) Direct Matrix Entry Version

For programs such as NASTRAN that accept direct entries to the assembled global dynamic stiffness matrix ($[K_{dd}]$, in NASTRAN) the components of equation (9) can be entered directly with DMIG cards. Since NASTRAN accepts complex entries, there is no problem with inserting both the real and imaginary parts of the $[\tilde{K}]'$ matrix into NASTRAN.

For finite element codes other than NASTRAN that do not accept a complex stiffness entry directly,it can be done indirectly by inserting the real part of $[\tilde{K}]'$ through the usual structural stiffness entry, $[K]$, and the imaginary part of $[\tilde{K}]'$ through the damping matrix, $[C]$, after dividing img.pt($[\tilde{K}]'$) by ω_1.

b) Spring-Damper Entry Version

The matrix $[\tilde{K}]$, (before coordinate transformation) can be built from simple

lumped parameter springs and damper as illustrated in Figure 3b. The idea is to assign values to the springs and dampers, so that the assembled [K] matrix is formed. By inspection of Figure 3b, the local element dynamic stiffness is

$$[\tilde{K}] = \begin{bmatrix} (K_\ell + K_m) + i\omega (C_m + C_\ell) & -K_m - i\omega C_m \\ \text{SYMM} & (K_r + K_m) + i\omega (C_m + C_r) \end{bmatrix} \quad (10)$$

Upon equating equations (8) and (10) in conjunction with equation (7), we arrive at the following constants for the single frequency lumped parameter model:

$$\begin{aligned} K_m &= -\bar{K}^r_{LR}\bar{A} & C_\ell &= (\bar{K}^i_{LL} + \bar{K}^i_{LR})\bar{A}/\omega \\ C_m &= -\bar{K}^i_{LR}\bar{A}/\omega & K_r &= (\bar{K}^r_{RR} + \bar{K}^r_{LR})\bar{A} \\ K_\ell &= (\bar{K}^r_{LL} + \bar{K}^r_{LR})\bar{A} & C_r &= (\bar{K}^i_{RR} + \bar{K}^i_{LR})\bar{A}/\omega \end{aligned} \quad (11)$$

where $\bar{A} = A_n/A_p$, is the nodal area to patch area ratio.

In the NASTRAN program, these lumped parameters are entered via CELAS2 and CDAMP2 cards. When the elements are not in line with the global axis, coordinate transformations are involved, i.e. involving equation (9)--or--employing different reference frames for each element using CORD1R cards.

c.) Three Rod Version

The three rod element (made from CONROD elements in NASTRAN) shown in Figure 3b is an alternate procedure to install the desired equation (9) dynamic stiffness. The rods, properly sized, will generate the same dynamic stiffness matrices as either of the two mentioned ones, but has the advantage that the coordinate transformations, should they be needed, are taken into account automatically in the finite element program. The same dynamic stiffness realized by the Figure 3b model can be achieved with the Figure 3c three massless rod model by using the following rod properties shown in Table 1.

TABLE 1 Single Frequency Rod Properties

	Mass Density ρ	Young's Modulus E	Poisson's Ratio ν	Loss Factor η	Cross Sec Area A	Rod Length L
Left rod	0	K_ℓ	0	$\omega C_\ell/K_\ell$	T	T
Middle rod	0	K_m	0	$\omega C_m/K_m$	T	T
Right rod	0	K_r	0	$\omega C_r/K_r$	T	T

The stiffness of a rod is AE/L, and the damping matrix is η AE/L, thus it can be seen how the Figure 3b and 3c models result in equivalent dynamic stiffness matrices. The 6 Constants K_ℓ,. . .C_r are still computed using Equation 11. The material properties ρ, E, ν, η, A appear on the CONROD and MAT1 cards in

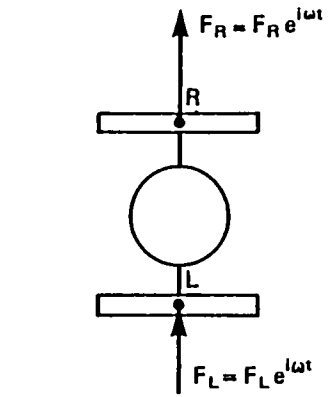

$$\begin{Bmatrix} \bar{F}_L \\ \hline \bar{F}_R \end{Bmatrix} = \left[\begin{array}{c|c} \bar{K}_{LL} & \bar{K}_{LR} \\ \hline \bar{K}_{RL} & \bar{K}_{RR} \end{array}\right] \begin{Bmatrix} \bar{U}_L \\ \hline \bar{U}_R \end{Bmatrix}$$

a) DIRECT MATRIX ENTRY VERSION

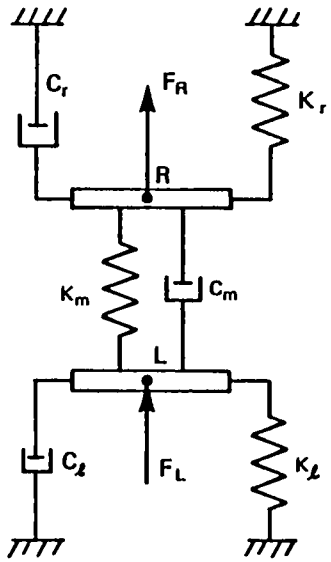

b) SPRING - DAMPER VERSION

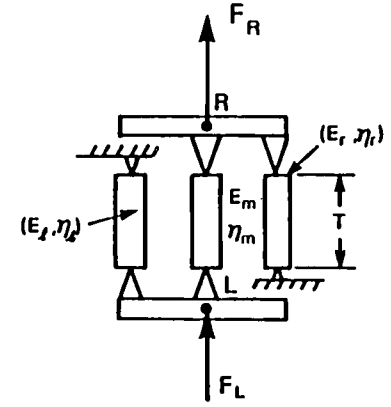

$\rho_\ell = \rho_m = \rho_r = 0$

c) THREE MASSLESS RODS VERSION

FIGURE - 3 SINGLE FREQUENCY IMPEDENCE ELEMENT

NASTRAN, however length T is computed by the program as the distance between terminal nodes R, and L in Figure 2. The user must be sure to enter a T in the area slot that is consistent with this length! Also care must be taken to ground out one end of the left and right rod as shown schematically in Figure 3c. See Table 2 comments for entering a negative modulus, E.

Two-Frequency Lumped Parameter Element

The object of this macroscopic element is to have a single element represent the dynamic stiffness of the patch over a limited range of frequencies, without having to change the parameter constants. This would have use as a convenience feature when performing a frequency sweep analysis--or--may be of use in a transient type solution, where the model is expected to be accurate over a narrow band of frequencies.

a.) Mass-Spring-Damper Version

The element local dynamic stiffness matrix for the model shown in Figure 4b is given by the relation

$$[\tilde{K}] = \begin{bmatrix} (K_\ell + K_m) - \omega^2(M_\ell + M_m\beta_1) + i\left(\omega(C_m + C_\ell) + K_\ell^c + K_m^c\right) & -(K_m + M\beta\omega^2) - i\left(C_m\omega + K_m^c\right) \\ \text{SYMM} & (K_r + K_m) - \omega^2(M_r + M\beta_1) + i\left(\omega(C_m + C_r) + K_r^c + K_m^c\right) \end{bmatrix} \quad (12)$$

The structure of equation (12) permits one to vary both the real and imaginary parts of the three main entries of the $[\tilde{K}]$ matrix by changing the frequency ω. Note that had a lumped mass been used for the center mass element, the real part of the K_{LR} entry would not depend on frequency. A set of twelve equations and twelve unknowns can be set up to solve for twelve unknown lumped parameters K_ℓ, ...M_m appearing in equation (12). The system of equations is obtained by equating corresponding real and imaginary parts of equation (12) and (8) at the first desired frequency, ω_1 and again equating equations (12) and (8) evaluated at the second desired frequency, ω_2. Let the entries of equation (7) with a subscript 1 refer to the "run-a", "run-b" pair of stiffness generating runs described earlier at frequency (i.e. $\bar{K}_{LL1}$,...$\bar{K}_{RR1}$) and similarly let entries of equation (7) with subscripts 2 refer to the "run-a", "run-b" pair run at frequency ω_2 (i.e. $\bar{K}_{LL2}$,...$\bar{K}_{RR2}$. Solving these twelve weakly coupled equations, the following twelve results are obtained for the unknown lumped parameters, K_m ...K_r^c

$$K_m = (\omega_2^2 \bar{K}^r_{LR1} - \omega_1^2 \bar{K}^r_{LR2})/\Delta_2$$

$$M_m = -(\bar{K}^r_{LR1} - \bar{K}^r_{LR2})/(\beta_2 \Delta_2)$$

$$C_m = (\bar{K}^i_{LR2} - \bar{K}^i_{LR1})/\Delta_1$$

$$K^c_m = (\omega_2 \bar{K}^i_{LR1} - \omega_1 \bar{K}^i_{LR2})/\Delta_1$$

$$K_\ell = (\omega_1^2 B_2 - \omega_2^2 B_1)/\Delta_2$$

$$M_\ell = (B_2 - B_1)/\Delta_2$$

$$C_\ell = (D_1 - D_2)/\Delta_1$$

$$K^c_\ell = (\omega_1 D_2 - \omega_2 D_1)/\Delta_1$$

$$K_r = (\omega_1^2 F_2 - \omega_2^2 F_1)/\Delta_2$$

$$M_r = (F_2 - F_1)/\Delta_2$$

$$C_r = (G_1 - G_2)/\Delta_1$$

$$K^c_r = (\omega_1 G_2 - \omega_2 G_1)/\Delta_1$$

where $\Delta_1 = (\omega_1 - \omega_2)/\bar{A}$ $\quad \Delta_2 = (\omega_1^2 - \omega_2^2)/\bar{A}$ $\quad \bar{A} = A_n/A_p$ (13)

$$B_1 = \bar{K}^r_{LL1} - K_m + M_m \omega_1^2 \beta_1$$

$$B_2 = \bar{K}^r_{LL2} - K_m + M_m \omega_2^2 \beta_1$$

$$D_1 = \bar{K}^i_{LL1} - \omega_1 C_m - K^c_m$$

$$D_2 = \bar{K}^i_{LL2} - \omega_2 C_m - K^c_m$$

$$F_1 = \bar{K}^r_{RR1} - K_m + M_m \omega_1^2 \beta_1$$

$$F_2 = \bar{K}^r_{RR2} - K_m + M_m \omega_2^2 \beta_1$$

$$G_1 = \bar{K}^i_{RR1} - \omega_1 C_m - K^c_m$$

$$G_2 = \bar{K}^i_{RR2} - \omega_2 C_m - K^c_m$$

It is noted that β_1 and β_2 are not unknowns, but rather free parameters that can be selected by the user. However, when using the six rod version discussed later, one must use the β_1, β_2 factors corresponding to the consistent mass matrix being employed by the finite element program being used. The implementation of the model shown in Figure (4b) cannot be achieved, due to the fact we need a complex spring, iK_r^c, which is not possible to enter with say an CELAS2 card in NASTRAN. Instead, it can be realized either with the direct matrix entry option or with a six rod element shown in Figure 4c as explained next.

b) Direct Matrix Entry Version

Once the basic lumped parameters have been computed, via equation (13), the element matrix in equation (12) can be entered directly with DMIG cards for the assembled global NASTRAN $[K_{dd}]$ matrix, $[B_{dd}]$ and $[M_{dd}]$ matrices. Again letting the notation L, R denote the left right terminal node notation, we have

$$\left.\begin{aligned} [K_{dd}]_{LL} &= (K_\ell + K_m),\ i(K_\ell^c + K_m^c) \\ [K_{dd}]_{LR} &= -K_m,\ -iK_m^c \\ [K_{dd}]_{RR} &= (K_r + K_m),\ i(K_r^c + K_m^c) \end{aligned}\right\} \text{(enter as complex on DMIG card)}$$

$$[B_{dd}]_{LL} = C_m + C_\ell \qquad (14)$$

$$[B_{dd}]_{LR} = -C_m \qquad [B_{dd}]_{RR} = C_m + C_r$$

$$[M_{dd}]_{LL} = M_\ell + M_m\beta_1$$

$$[M_{dd}]_{LR} = M_m\beta_2$$

$$[M_{dd}]_{RR} = M_r + M_m\beta_1$$

As in the previous single frequency model, step to account for the coordinate transformation must be taken where applicable. The next 6-rod model will handle the coordinate transformations automatically.

c) Six Rod Element Version

A constant mass viscoelastic rod element with viscoelastic damping, η, has a dynamic stiffness matrix of the form:

$$[\bar{K}]_{rod} = \begin{bmatrix} (AE/\ell - m\omega^2\beta_1) + i\eta AE/\ell & -(AE/\ell + m\omega^2\beta_2) - i\eta AE/\ell \\ \text{SYMM} & (\frac{AE}{\ell} - m\omega^2\beta_1) + i\eta AE/\ell \end{bmatrix} \qquad (15)$$

where A is the rod cross section area; $m = A\rho\ell$ the total rod mass; ℓ is the rod

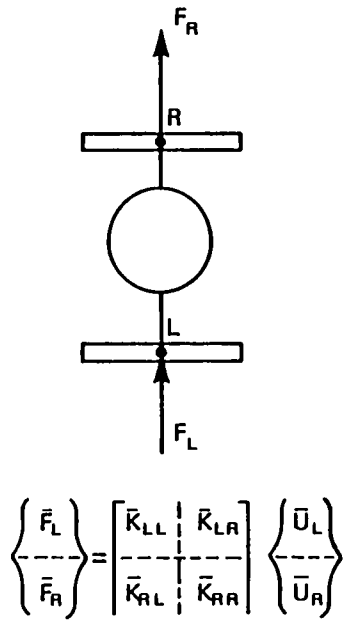

a) DIRECT MATRIX ENTRY VERSION

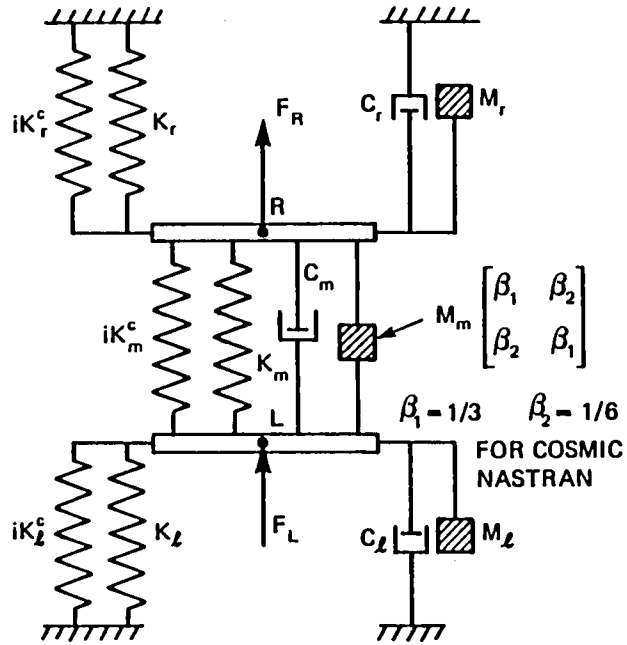

b) MASS - SPRING - DAMPER VERSION

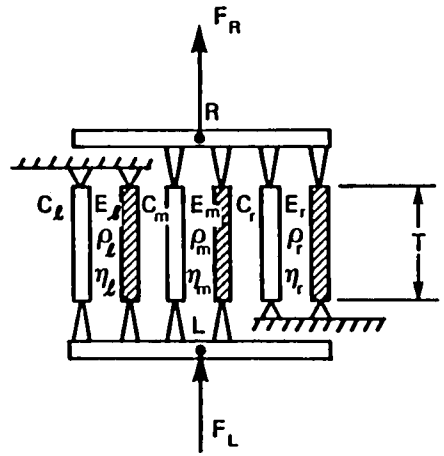

c) SIX - RODS VERSION

SHADED — CONSISTANT MASS VISCOELASTIC ROD
UNSHADED — VISCOUS DAMPER ROD

FIGURE - 4 TWO-FREQUENCY IMPEDENCE ELEMENT

length, E the modulus of elasticity and β_1 , β_2 are the mass distribution factors. It should be noted that the β factors may be different versions of NASTRAN (see note below Table 2).

Upon comparing equation (14) to equation (15), a set of equivalent rods can be defined to correspond exactly to the Figure 4b configuration. Table 2 below give the equivalent constants

TABLE 2 Two Frequency Rod Properties

	Mass density ρ	Young's Modulus E	Poisson's Ratio ν	Loss Factor η	Lumped Damping Constant C	Cross Sectional Area A	Rod Length (Indirect input) L
left viscoelastic rod	$M_\ell/(\beta_1 T^2)$	K_ℓ	0	K_ℓ^c/K_ℓ	—	T	T
left damper rod	--	--	—	--	C_ℓ	--	T
mid viscoelastic rod	M_m/T^2	K_m	0	K_m^c/K_m	—	T	T
mid damper rod	--	--	--	--	C_m	--	T
right viscoelastic rod	$M_r/(\beta_1 T^2)$	K_r	0	K_r^c/K_r	--	T	T
right damper rod	--	--	--	—	C_r	--	T

NOTE:
- For COSMIC NATRAN $\beta_1 = 1/3$ $\beta_2 = 1/6$
- For MSC NASTRAN $\beta_1 = 5/12$ $\beta_2 = 1/12$

In both COSMIC or MSC NASTRAN, the viscoelastic rods are implemented with CONROD elements (with GE as the loss factor on a MAT1 card) and the damper rods are implemented with CVISC elements where the lumped parameter damping constant is directly entered on the corresponding PVISC property card. The twelve basic constants K_m ...M_r given by equation (13) are the raw data that make up the 6 rod model. The rod length is not direct input to the 6 rods, but is rather computed automatically by the finite element program based on the length between "L" node and "R" node. It is important that the, T, length factor used for the dummy rod density and dummy rod area in Table 2 must be totally consistent with the distance between nodes L and R. Also care must be taken to ground out one end of the left CONROD and CVISC elements and also one end of the right CONROD and CVISC elements. Should E be negative, leave it blank and instead use a dummy positive shear modulus, G, and corresponding negative Poisson's ratio that corresponds to the desired negative E. For example, set G = |E| and set ν = -1.5.

DEMONSTRATION EXAMPLE PROBLEM

A soft inhomogeneous viscoelastic layer is attached to a stiff backing plate as shown in Figure 5a. The submerged sheet is a generic configuration that does not correspond to any particular real application, and is included here only to give some idea of the accuracy of the solution methodology in a simple application. Further, the details of the model are too lengthy to give here, and are beyond the intent of this demonstration problem. The example problem is kept simple by assuming the inhomogeneities are planar, thus permitting us to use two dimensional elements having a unit depth for the D variable of Figure 1a. The inhomogeneities were simulated by simply assigning different material constants (Young's modulus, mass density and dissipation loss factor) to soft layer finite elements in Figure 5b in the region marked soft layer. The inhomogeneities were distributed mainly in nonlayered patterns.

In the sample problem, the two frequency element of Figure 4 was used. The TxW region in Figure 5b, was used to generate the macroscopic dynamic stiffness versus frequencies using the "run-a", "run-b" procedure described earlier in the paper, in conjunction with the stiffness generator procedure illustrated in Figure 1b. The results of these 5x2 runs are shown in Figure 6, where the frequencies, ω, are normalized (divided) by (C_a/W) where C_a is the incident side acoustic medium wave speed. Further, the dynamic stiffnesses are normalized (divided) by the patch area, $A_p = WD$.

We arbitrarily selected the Figure 4 two frequency model to work at normalized frequencies of .733 and .837, as shown by the triangle markers in Figure 6. We purposely did not make the spread greater, so that some idea of how well the model would work in between the forced points could be examined. For example, the dashed line shown connecting the two forced points in Figure 6 ($\bar{K}_{RR}$ plot) represents the dynamic stiffness of the $\bar{K}_{RR}$ component of the Figure 4 two-frequency model. Since we have not forced the dynamic stiffness to be exactly equal to the patch model, some error can be expected in the response results if the two frequency model is used at the in between non forced frequency points.

The direct stiffness, mass, and damping via DMIG cards option (i.e. with equations 14) was used to implement the Figure 4 two-frequency model. The 6-bars model was not tried, because the CVISC viscous damping elements do not always assemble properly on the DEC VAX SERIES MODEL 11/780, April, 1984 release of NASTRAN. Hopefully these elements will be fixed in future releases.

The Figure 5b finite model was subject to an incident harmonic wave of strength P_o at the two normalized frequencies of .733 and .837 corresponding to the forced frequencies of the Figure 4 two-frequency model. The finite element model was first run with the full microscopic finite element representation for the soft layer (e.g. the soft inhomogeneous layer is represented with 398 quadrilateral and triangular elements)--and--secondly was rerun with one single Figure 4 type element replacing the original 398 finite elements. The reflected pressure at the far end of the finite element model was used to compare results. The results are shown in Table 3.

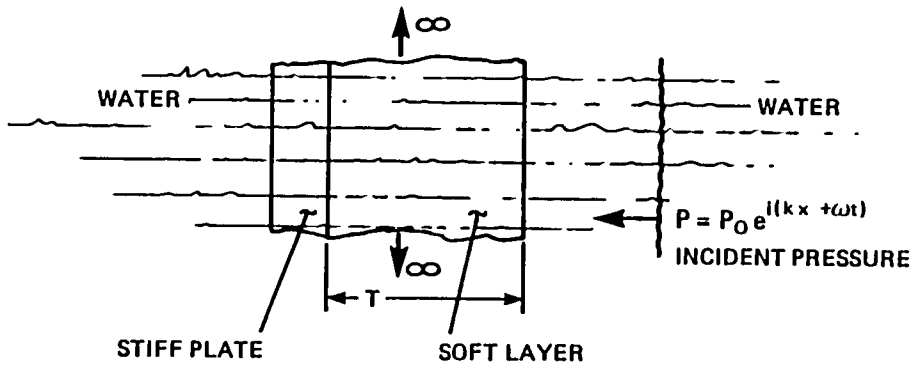

a) SUBMERGED FLAT PLATE

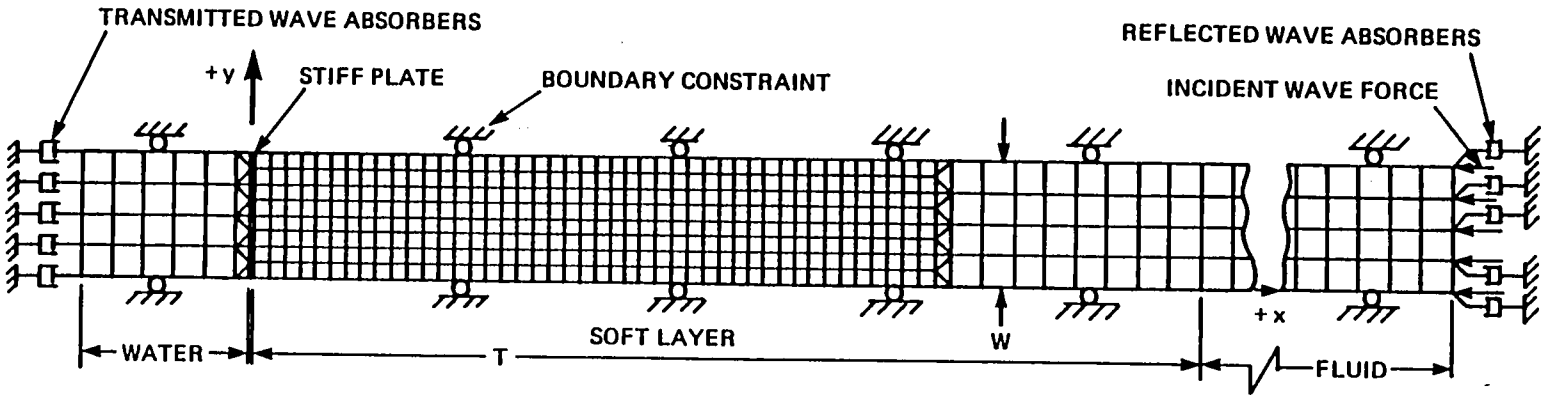

- 398 ELEMENTS FOR SOFT LAYER ALONE
- 856 ELEMENTS (CQDMEM, (TRMEM, CBAR)) (ENTIRE MODEL)
- 588 GRID POINTS

W = WIDTH OF REPRESENTATIVE MICROSCOPIC PATCH OF SOFT LAYER

b) FINITE ELEMENT MODEL

FIGURE - 5 SAMPLE NON-HOMOGENOUS MICROSCOPIC FINITE ELEMENT MODEL

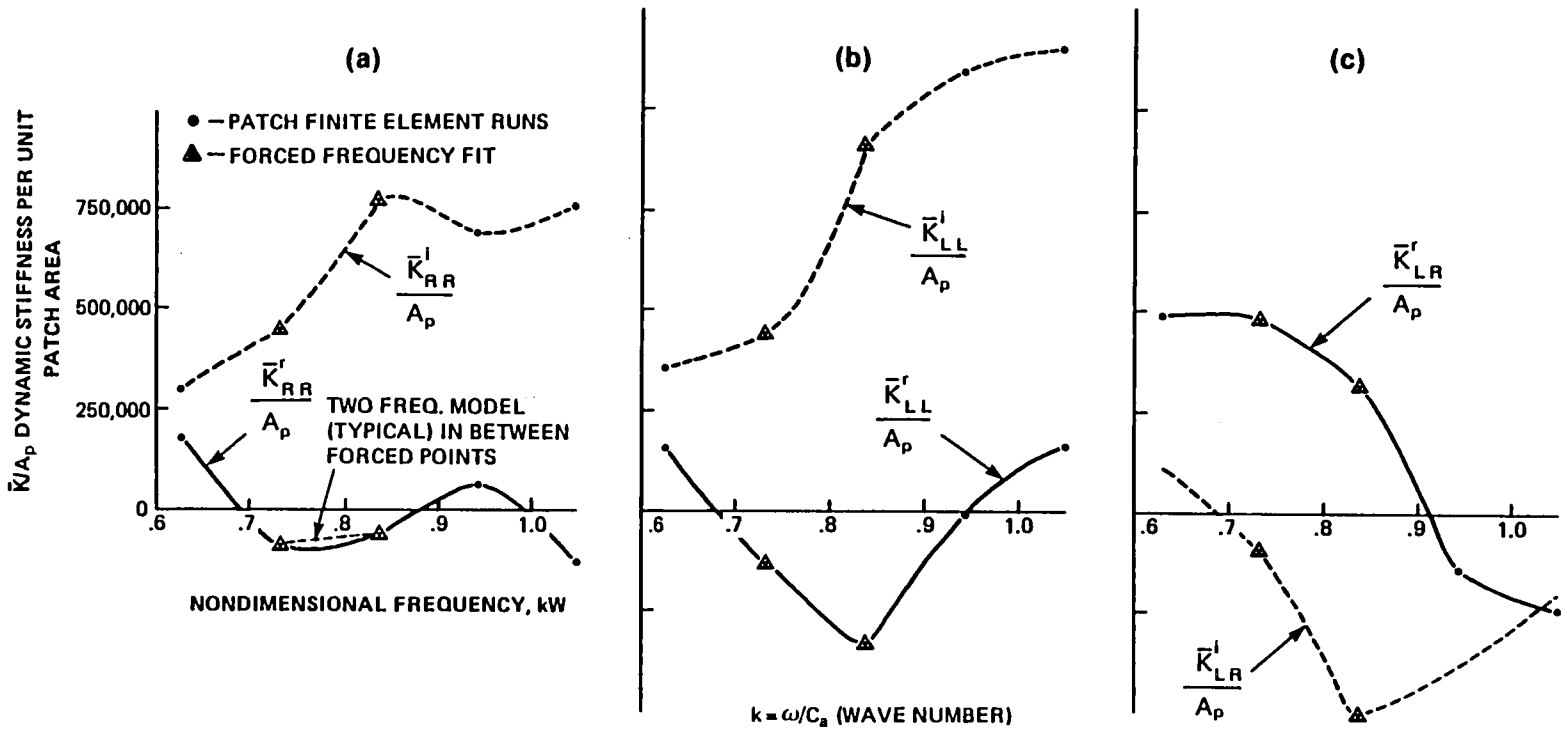

FIGURE - 6 MACROSCOPIC DYNAMIC STIFFNESS VS. NONDIMENSIONAL FREQUENCY

TABLE 3 Comparison of Results (REFLECTED PRESSURE/ P_o)

$\omega W/C_a$	398 Finite Element Model	1-Macroscopic element
.733	.1782	.1784 ← Two freq model
.785	.1357	.1032 designed to work
.837	.05476	.05476 ← at these two values

CONCLUDING REMARKS

The method presented provides a simple means for representing complicated finite element models of inhomogeneous viscoelastic layers with simplier elements, that are designed to work at specific frequencies. Preliminary results for the two-frequency macroscopic element on the simple flat sheet showed good results for the reflected pressure when compared to the same analysis using a full blown microscopic finite element implementation. The results were not quite as good, 23.9% error, for the comparison involving the "in between frequency run". However, the macroscopic elements are not specifically designed to work at the intermediate frequencies, and therefore it would be a windfall situation had they worked there as well. For example if the spread between the two frequencies were made larger, where the second forced frequency point in Figure 6 had been say, 1.0 instead of the .837, a substantial misfit in the dynamic stiffness would be expected due to the curved shape of $\bar{K}'_{LL}$, particularly in the range $0.8<kW<0.9$. If results are desired in this range, new lumped parameters should be recomputed and a new 2-frequency model be used that is valid for the desired frequencies.

The next future checkout application of the macroscopic elements should be for a curved surface of the type shown in Figure 2. It must be remembered that the macroscopic elements are not intended to represent the physics of the actual dynamic system existing between the L, R terminal nodes but rather simply represent the impedance of the actual inhomogeneous soft layer at those two frequencies.

REFERENCES

1. Pritz, T., "Transfer Function Method for Investigating the Complex Modulus of Acoustic Materials: Spring-Like Specimen", Journal of Sound and Vibrations, 72(3), 1980.

2. Khaikovich, I. M. and Khalfin, L. A., "The Effective Dynamic Parameters for Sound Propagation In Inhomogeneous Media", Soviet Physics (Acoustics), 4(3), July 1958.

3. Toulis, W. J., "Acoustic Refraction and Scattering with Compliant Elements .II. Analysis:, J. Acoustic Soc. Am. 29 (9) Sept. 1957.

4. George, J. and Uberall, H., "Approximate Methods to Describe the Reflections From Cylinders and Spheres With Complex Impedance, J. Acoustic Soc. Am. GS (1), Jan. 1979.

5. Stephens, R. W. B., Physics of Plastic, ed. P. Ritchie, D. VanNostrand Co., Princeton, 1965 (Chapter 9).

6. Kalinowski, A. J., and Nebelung, "Solution of Axisymmetric Fluid Structure Interaction Problem with NASTRAN", 10th NASTRAN Users' Colloquium (NASA Cof. Pub. 2249), May 1982.

7. Everstine, G. C., Schroeder, E. A. and Marcus, M. S., "The Dynamic Analysis of Submerged Structures", 4th NASTRAN Users' Colloquium, (NASA Conf. Pub. TMX-3278), 1975.

8. Kalinowski, A. J., "A Survey of Finite Element-Related Techniques As Applied to Acoustic Propagation In the Ocean" Parts I & II, The Shock and Vibration Digest, Vol II (3,4), March, April 1979.

9. Kalinowski, A. J., "Geometrically Corrected Viscous Boundaries For Steady State Acoustic Scattering and Radiation Problems", Proceedings of ASME Winter Annual Meeting, Nov. 1981, ASME Publication AMD-Vol. 46.

10. Kalinowski, A. J., "Steady State Solutions to Dynamically Loaded Periodic Structures," 8th NASTRAN Users' Colloquium, Oct. 1979.

11. Przemieniecki, J. S., Theory of Matrix Structural Analysis, McGraw Hill, 1968.